The Effect of an Organic Surfactant on the Liquid−Vapor Interface of an Electrolyte Solution

ARTICLE *in* THE JOURNAL OF PHYSICAL CHEMISTRY C · SEPTEMBER 2007

Impact Factor: 4.77 · DOI: 10.1021/jp073078b

The Effect of an Organic Surfactant on the Liquid−Vapor Interface of an Electrolyte Solution

Maria J. Krisch,[†] Raffaella D'Auria,[†] Matthew A. Brown, Douglas J. Tobias,* and John C. Hemminger*

Department of Chemistry and AirUCI, University of California at Irvine, Irvine, California 92697

Markus Ammann

Laboratory of Radio- and Environmental Chemistry, Paul Scherrer Institute, CH-5232 Villigen, Switzerland

David E. Starr[‡] and Hendrik Bluhm

Lawrence Berkeley National Laboratory, Mail Stop 6R2100, One Cyclotron Road, Berkeley, California 94720

Received: April 21, 2007; In Final Form: July 2, 2007

Insight into ion behavior at mixed organic/aqueous liquid surfaces is crucial for understanding the chemistry of atmospheric aerosols, which frequently contain mixtures of water, electrolytes, and organics. The addition of 1-butanol to an aqueous potassium iodide solution modifies the interfacial profile of ions at the liquid−vapor interface. Our experiments probe atomic composition at the liquid surface with ambient pressure X-ray photoelectron spectroscopy. Photoelectron kinetic energies are varied to produce a depth profile of the liquid−vapor interface. Molecular dynamics simulations of butanol in an aqueous electrolyte solution are used to develop a detailed understanding of the ion−solvent interactions in the interfacial region. Our previous work on pure aqueous salt solutions observed substantial ion concentrations at the liquid−vapor interface and an increased anion/cation ratio at the interface. A question has arisen as to whether covering the surface with an organic monolayer might change or suppress the interfacial ion concentrations. We observe that the direct interaction of both the cation and the anion with the butanol leads to changes in the ion concentrations in the region of the liquid interface. Substantial ion concentrations are still observed in the interfacial region in the presence of butanol. However, we do find that the presence of the butanol reduces the previously observed anion/cation separation in the interfacial region.

Introduction

Air−water interfaces play an important role in atmospheric chemistry due to the abundance of high surface-area aerosol in the atmosphere. Both theory and experiment are converging on a coherent picture of the air−water interface of aqueous salt solutions in which certain ions are expected to segregate to the surface. This result may affect reaction kinetics in marine aerosol systems that contain dissolved salts. To investigate the atmospheric implications of this finding, it is essential to account for the fact that a substantial amount of marine aerosol appears to be made up of organics. Aerosol composition varies widely, depending upon variables such as aerosol size, location, and the time of year.[1] In this study, we extend our understanding of aqueous salt solution interfaces by studying a more complex, atmospherically relevant model system: a ternary mixture of water, KI, and 1-butanol.

Extensive work has recently focused on characterizing the behavior of ions at the liquid−vapor interface. Interest in the field was motivated by two experiments that observed unexpectedly high reaction rates between halide ions in solution and impinging gases.[2,3] One way to explain the measured reaction rates is to postulate enhanced ion concentrations at the interface. Initially, however, this idea appeared to contradict the decades-old perception that image charges repel ions from the air−water interface. Subsequent molecular dynamics (MD) simulations revealed that when polarizability is incorporated into simulations of ions in water, certain ions show enhanced concentrations at the interface (see review by Jungwirth and Tobias[4]). Ions are thought to surface segregate, in part, because of the asymmetry of the air−water interface. This asymmetric environment induces a dipole in polarizable ions that is stabilized by the surrounding solvent. Because ions are only partially solvated at the interface, this dipole effect competes with the full solvation offered in the bulk of the solution.

The prediction of enhanced interfacial ion concentrations generated an intense experimental effort to characterize the amount of ions at the air−water interface of aqueous salt solutions. Our group used ambient pressure X-ray photoelectron spectroscopy (XPS) to directly measure the depth profile of ions at the surface of aqueous salt solutions, observing surface enhancement of I^- and Br^- in aqueous KI and KBr solutions, respectively.[5] Second harmonic generation spectroscopy experiments by the Saykally group utilized charge-transfer-to-solvent resonances in the ions of interest and were also able to observe surface segregation of ions (see, for example, refs 6,7). Vibrational sum frequency second harmonic generation measurements showed changes in water structure consistent with an enhanced concentration of ions at the interface (this technique

* To whom correspondence should be addressed. (J.C.H.) E-mail: jchemmin@uci.edu. Phone: 949-824-6022. Fax: 949-824-2261. (D.J.T.) E-mail: dtobias@uci.edu. Phone: 949-824-4295. Fax: 949-824-8571.

[†] M.J.K. and R.D. contributed equally to this work.

[‡] Current address: Center for Functional Nanomaterials, Brookhaven National Laboratory, Upton, New York, 11973.

10.1021/jp073078b CCC: $37.00
Published on Web 08/18/2007

was used in both the Allen[8] and Richmond[9] groups). Several valence band photoemission experiments of liquid jets also examined aqueous salt solutions (see review by Winter and Faubel[10]). A recent paper has reconciled the current understanding that surface segregation can occur for polarizable anions with a thermodynamic treatment of surface tension measurements for aqueous electrolyte solutions, data that were initially interpreted to imply a repulsion of ions from the interface.[11] Recent experiments from our group have also shown that Br^- preferentially segregates to the liquid−vapor interface of mixed NaCl/NaBr solutions.[12] This preferential segregation has also been predicted by MD simulations.[13]

In the work described here, we present the first results that show the impact of an organic on the surface ion concentrations of an aqueous KI solution. Butanol is an attractive choice of model organic because a substantial body of work characterizes the liquid−vapor interface in salt-free solutions of butanol and water. Numerous groups have measured the surface tension of butanol−water solutions.[14] The surface excess of butanol at the liquid−vapor interface has been characterized by surface tension[14] and neutron reflectivity[15] measurements. Monte Carlo simulations by Chen et al. found substantial changes in the bonding and orientation of interfacial butanol and water in mixtures of butanol saturated in water and water saturated in butanol, as compared to neat solutions of either chemical.[16] Their conclusion that the surface orientation of butanol is more perpendicular for small amounts of butanol in water than for neat butanol is consistent with evidence from surface potential experiments.[17] Butanol is soluble in water, with a Henry's law constant of 130 M/atm at 298 K.[18] Although the butanol−water systems studied above are similar to the model system used here, the presence of salt in high concentrations is expected to modify the properties of the solution. In particular, KI is known to be a "salting out" agent with respect to butanol, making butanol less soluble and more surface active in a salt solution than in pure water.[19] In this paper, we also present surface tension measurements of butanol in a saturated KI solution to characterize changes in the surface excess of butanol due to the presence of salt.

The structure of a typical mixed-component aerosol is a subject of much active research. A core−shell model in which surface-active organics reside at the outside of aerosol liquid droplets has been proposed.[20,21] In cases where the organic is an amphiphilic surfactant, this can be thought of as a "reverse micelle" model of aerosol structure. Experimental confirmation exists for this model in only a few liquid-phase systems. Mixed droplets of butanol and water (without salt) were possibly the first system in which a core−shell structure was observed experimentally through small angle neutron scattering experiments of water−butanol nanodroplets.[22] This experiment was linked to a supporting density functional study on water−pentanol droplets that predicted a core−shell structure for certain concentration ranges of alcohol and water.[23] Recent experiments performing Raman scattering of droplets contained in an optical trap found that ethanol and aqueous sodium chloride are homogeneously mixed while droplets of aqueous sodium chloride and decane appeared to have roughly a core−shell structure.[24] Time-of-flight−secondary-ion mass spectrometry measurements have also shown evidence for organic coatings on aerosols collected directly in the field, although these experiments may not directly extrapolate to undisturbed, liquid-phase systems.[25]

While a core−shell structure has been observed in selected cases, alternate models of the distribution of organics in aerosols exist and may apply in other systems or conditions. Tabazadeh pointed out that under many concentration regimes, surfactants may preferentially form micelles in solution instead of segregating to the surface and forming reverse micelles.[26] Another model comes from groups examining aqueous solutions of soluble surfactants and ethylene glycol through evaporation and Brewster angle microscopy.[27,28] These researchers conclude from their data that bilamellar aggregates form slightly under the surface of the solutions. Finally, we note that aerosol structure may change over time. Recent experiments have demonstrated that reaction with atmospheric oxidants can substantially modify a surface active organic film over a liquid if soluble reaction products go into solution.[29] Despite the variety of aerosol models, it is clear that the core−shell picture is a good representation of butanol−water mixtures, making our model system a well-characterized starting point for experiments.

In this paper, we report the results of ambient pressure XPS measurements on ternary solutions of water, KI, and butanol. We examine elemental composition as a function of depth into solution, finding suppression of the surface enhanced anion/cation ratio that is observed in solutions of KI in pure water. MD simulations of mixtures of water, NaI, and a variety of concentrations of butanol also show suppression of the enhanced anion/cation ratio at the interface of the solution and elucidate the mechanism underlying this suppression. As a result of direct ion−butanol interactions, both the anion and cation exist at similar concentrations in the region of the liquid−vapor interface.

Experimental Procedures

A. Ambient Pressure XPS. The experiments presented here used ambient pressure XPS with synchrotron light as a source of X-rays to measure the surface composition of saturated KI solutions in the presence and absence of butanol. Measurements were made at the Molecular Environmental Sciences beamline (11.0.2) of the Advanced Light Source (ALS) at Lawrence Berkeley National Laboratory.[30] The experimental apparatus utilizes a detection system similar to a prototype that is described in the literature.[31] Briefly, the apparatus uses a three-stage differentially pumped electrostatic lens and hemispherical analyzer to collect photoelectrons from samples in chamber pressures up to a few Torr. Electrostatic lenses refocus the electrons between each differentially pumped stage. To minimize the attenuation of the signal due to scattering of electrons by gas-phase molecules, the distance between the sample and the collection aperture (0.3 mm diameter) is kept small, on the order of 0.5 mm, to reduce the volume of gas seen by the ejected electrons. Because the incident photon beam also irradiates some gas volume in front of the sample surface, electrons from gas-phase and condensed-phase species are collected simultaneously.

The incident X-rays enter the chamber through a 100 nm thick silicon nitride window (active area 0.5×0.5 mm^2) situated 1.5 centimeters from the sample. The angle between the incident X-rays and the photoelectron collection is 54.7° (i.e., the "magic angle"). Measurements of the X-ray flux near the sample position are repeated regularly with a photodiode with known quantum efficiency.

Single-crystal KI from MaTecK was mounted on the sample holder with TorrSeal and cleaved in vacuum to expose the (100) face. "Dry" measurements to characterize the single crystal were taken at room temperature in 1.6 Torr water vapor ($\sim$ 8% relative humidity). To generate a liquid sample, the salt crystal was brought to deliquescence by cooling the crystal until the sample temperature and water pressure in the chamber reached

the deliquescence point of the crystal (78% relative humidity at −10 °C)[32] and the presence of solution was observed visually. All liquid spectra were collected from a salt-saturated liquid film covering a salt crystal. A circulating chiller and a Peltier block were used in combination to achieve sample temperatures between −9 and −12 °C, as read by a thermocouple attached to the bottom of the salt crystal. The crystal was kept as the coldest point in the chamber, and thus was the first location to condense water. Pressure and temperature were continuously monitored to ensure that the system remained at deliquescence (pressure was read by a baratron pressure gauge).

We used two approaches to form a multicomponent liquid mixture. First, we deliquesced the salt in the presence of water, took measurements of the saturated aqueous salt solution and then added gas-phase butanol into the chamber via a leak valve. In the second approach, gas-phase water and butanol were simultaneously added to the chamber via separate leak valves, and the sample was deliquesced in the presence of the butanol−water mixture. Our experimental results were not affected by the manner in which the solution was generated. In both approaches, the water pressure was approximately 1.6−1.7 Torr as measured on the baratron and approximately 0.2 Torr of butanol was added to the system. The C(1s) and O(1s) XPS peaks of gas-phase butanol and the O(1s) of water were also used to measure the gas-phase butanol concentration in the experiment.

We measured K(2p), I(4d), O(1s), and C(1s) XPS spectra at different photon energies to obtain depth profiles of K, I, O, and C, relying on the fact that the surface sensitivity in XPS arises from the inelastic mean free path (which is kinetic energy dependent) of the ejected photoelectrons. By tuning the incoming X-ray energy, we can vary the photoelectron kinetic energy. The resulting signal is integrated; we collect photoelectrons from a range of sample depths varying up to the maximum accessible escape depth at any given energy. To directly compare elemental ratios, we took sets of spectra corresponding to a single probing depth (same photoelectron kinetic energy) for all elements in rapid succession on one spot on the sample.

Beam damage from the incident X-rays is a concern in the iodide spectra, although the increased ionic mobility in liquids makes this less problematic in liquids than in solids. Iodide spectra were always taken first in any series of data and were often retaken at the end of the series to check for a loss in signal. We moved analysis spots on the sample frequently, not collecting more than two series in the same spot for the data presented here. We did not observe beam damage effects for K, C, and O.

In addition to visual monitoring of the sample, we have developed spectral criteria to ensure that any given measurement spot has not dried up due to movement and flowing of the salt solution. We have found that requiring a relative humidity of at least 78% in conjunction with the $O_{adsorbed}/K$ atomic composition ratio of 5−6 or above (expected ratios vary with the sample depth probed) is a robust measure to identify deliquesced spots on the sample. These criteria are verified by predictions of O/K ratios from MD simulations. The shape and intensity of the spectra also changes qualitatively in dry spots, and these changes can be correlated with the criteria mentioned above.

B. Surface Tension. We performed surface tension measurements with a NIMA pressure sensor (Model PS4) using a paper Wilhelmy plate. A Teflon trough contained sample volumes of 70−200 mL. A Teflon cover for the measuring trough minimized the effect of evaporation during data collection. We measured surface tension by drawing the liquid away from the Wilhelmy plate with an aspirator and comparing the lowest value of surface pressure to the reading from the free plate in air. MilliQ water with a resistance of 18.2 MΩ, KI salt of ACS reagent grade (≥99.0% purity), and ACS ReagentPlus butanol (99.9% purity) were used. The salt was further purified before each measurement by filtration through a Millex syringe filter (Millipore) followed by aspiration of the solution surface. All measurements were taken at 19.7 ± 0.3 °C. Surface tension values of KI in water solution were measured up to saturation concentrations and agreed reasonably with the high concentration KI measurements from Hård and Johansson (extrapolation of their data gave a 13% difference for the surface tension value at saturation).[33] Reference measurements on butanol−water mixtures agreed with literature values of surface tension as given in Harkins and Wampler[14] to within 4% or better.

C. MD Simulations. Classical MD simulations of a series of aqueous NaI solutions covered with an increasing number of 1-butanol molecules were performed using AMBER 8.[34] The systems investigated consisted of 864 water, 96 NaI, and *n* 1-butanol molecules in a 30 × 30 × 100 Å simulation unit cell subjected to three-dimensional periodic boundary conditions. In this "slab" geometry,[35,36] a region of "vapor" (vacuum) separates the periodic images in the extended *z* dimension, creating two liquid−vapor interfaces. A total of five different alcohol coverages were investigated, corresponding to $n = 0$, 32, 50, 72, and 98. The use of different amounts of alcohol allows for the investigation of changes in the liquid−vapor interfacial composition as the surface density of the organic layer is increased; moreover, it allows for the exploration of a range of possible experimental scenarios. The systems containing alcohol were prepared by placing $n/2$ 1-butanol molecules with their hydroxyl groups in contact with the two interfaces of a previously equilibrated 5 M NaI aqueous solution. Because of the large surface-to-volume ratio in the simulated systems and the enhanced presence of ions at the interfaces, the concentration of ions away from the interfaces in the slabs is slightly smaller than the concentration of an equivalent 5 M bulk system.

Following energy minimization, a 3 ns MD trajectory was generated for each system. The analysis was performed on the last 2 ns of each trajectory. The simulations were carried out at a temperature of 300 K using the method of weak coupling.[37] A time step of 1 fs was used to integrate the equation of motion, and the SHAKE algorithm[38] was used to constrain the lengths of bonds involving H atoms. The long-range electrostatic interactions were computed using the smooth particle mesh Ewald method,[39] and a cutoff of 12 Å was used to truncate the van der Waals interactions and the real part of the Ewald sum.

We used well-established polarizable force fields to represent water[40] and the ions.[41] We have carried out this theoretical investigation using sodium iodide instead of potassium iodide, which was used in the experimental part of the present study, because our group has had extensive experience in the use of the sodium cation force field. Preliminary tests that have been carried out for the salt water systems using available potassium cation force fields have shown no qualitative difference in the behavior of the ion density profiles. The 1-butanol model was adapted from the pairwise-additive Cornell et al. force field for amino acids.[41] In a simulation of a bulk system composed of 331 1-butanol molecules at constant temperature and pressure ($T = 300$ K, $p = 1$ atm), the resulting model gave an average

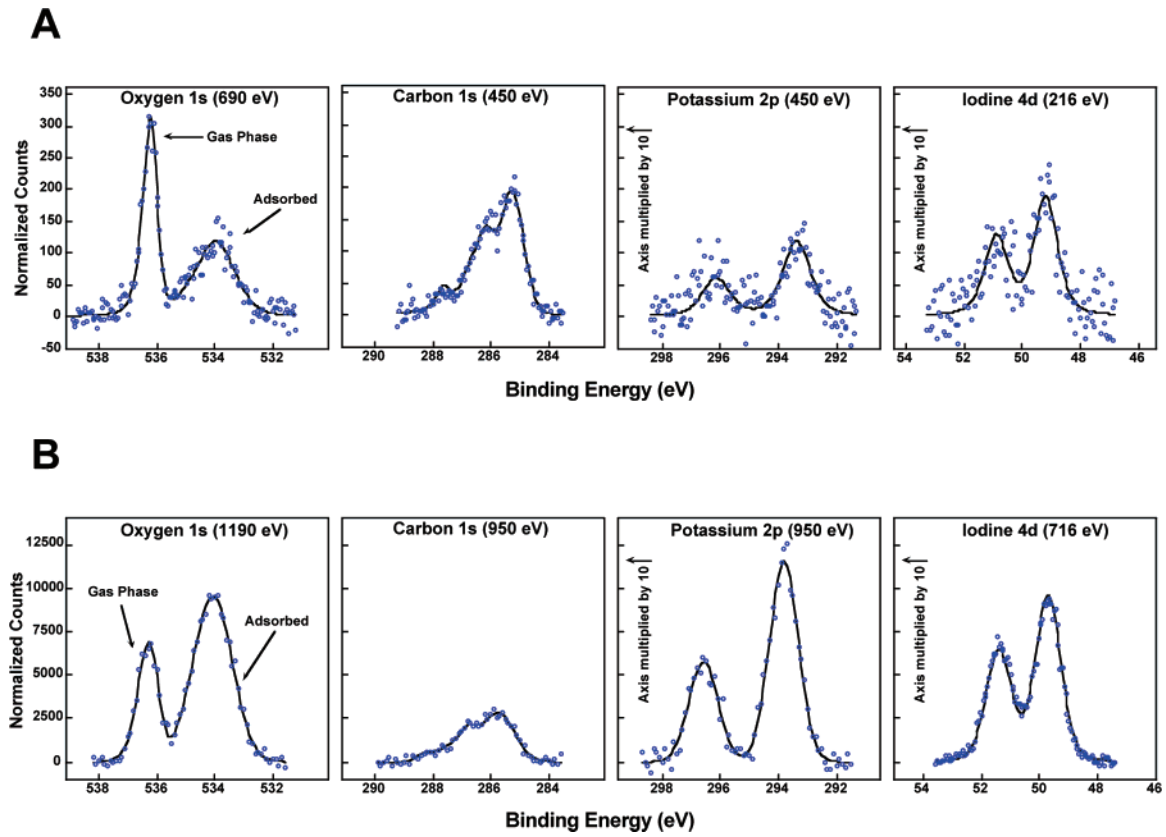

Figure 1. Set of representative ambient pressure XPS spectra of a KI−water−butanol solution taken at (a) low-photoelectron kinetic energy (150 eV) and (b) high-photoelectron kinetic energy (650 eV). The photon energies are given in parentheses for each spectrum. Each set of spectra was taken at the same spot on the sample in the order I, K/C, and O so that changes in experimental conditions were minimized. Fits to the data are shown as thick black lines (see the text for an explanation of the fitting procedure) and experimental data as circles. The spectra shown are background subtracted and normalized by X-ray flux and subshell photoionization cross section. The potassium and iodide signals at 150 eV represent a rough lower bound on the signal-to-noise for the spectra used.

density of 0.7946 g/cm^3, which differs by less than 2% from the experimental value.[42]

Results

Depth profiles of the liquid−vapor interface of a saturated KI solution with and without butanol were taken via ambient pressure XPS. Butanol was found to be surface active, as judged by the fact that carbon was enhanced at the interface in comparison to the bulk of the ternary KI−water−butanol solution. Enhancement of the iodide/potassium ratio at the interface, observed in the aqueous salt solution, was suppressed in the presence of butanol. This effect was also observed in MD simulations of NaI−water−butanol mixtures at various butanol concentrations, which show that both a cation, Na^+, and the I^- anion form distinct solvation shells around butanol.

A. Ambient Pressure XPS. *Spectral analysis.* We collected XPS spectra of the I(4d), O(1s), K(2p), and C(1s) peaks from the sample in the presence of pure water vapor or a mix of water vapor and butanol. The spectra were taken at a variety of photoelectron kinetic energies: 150, 190, 250, 280, 350, 450, 650, and 800 eV. Sample sets of spectra from photoelectron kinetic energies of 150 and 650 eV, which are more sensitive to the surface and bulk, respectively, are given in Figure 1 for a sample of KI deliquesced in the presence of both water and butanol. (The spectra at 800 eV photoelectron kinetic energy are most representative of the bulk, but we lacked sufficient signal to record oxygen at this energy so 650 eV corresponds to the deepest experimental probe depth where we have a complete set of data for all the relevant elements: I, O, K, C). To compare amounts of different elements, we normalize the integrated area of photoelectron signal by X-ray flux (calibrated at the beamline) and subshell photoionzation cross-sections.[43] The procedure used to fit the spectra to determine integrated areas is outlined in the following section.

Iodide 4d spectra, especially those from the salt solution in the absence of butanol, were fit to two iodide species using identical parameters for the line shapes (but not the areas). Investigation of the mechanism causing the appearance of the higher energy iodide peak is underway. The binding energy separation between the two iodide species is 1.4 ± 0.2 eV.

Oxygen spectra showed a strong signal from the gas phase, as well as a clearly separated adsorbed oxygen peak at lower binding energy. To characterize the gas-phase component, the sample was retracted and gas-phase spectra were collected. When butanol is present, the gas-phase spectra contain a small but distinct peak from the butanol oxygen that is 1.2 eV lower in binding energy than the large water oxygen 1s peak. The gas-phase XPS spectra also provided the basis for our determination of gas-phase butanol concentration by giving a ratio of water oxygen to butanol oxygen as discussed later. In spectra of the sample, the oxygen 1s peak gas-phase butanol overlaps with the water signal from the solution, so the butanol gas-phase peak was constrained to the parameters that were found in the neat gas-phase O(1s) spectra.

The carbon spectra in the presence of butanol also contained appreciable signal from both the gas and condensed phase. Gas-phase spectra were taken separately and used to determine fitting

parameters that gave a $C(1s)_{CH}$ to $C(1s)_{CO}$ ratio of 3:1 as expected for C_3H_9COH. The binding energy difference between the $C(1s)_{CH}$ and $C(1s)_{CO}$ peak positions was 1.5 eV. We fit all the carbon spectra with two doublets, one for the butanol gas-phase signal and another for the condensed-phase signal (the gas- and condensed-phase butanol C(1s) peaks overlapped substantially). By constraining the energy difference and relative areas within each doublet, we were able to obtain fits in which the peak positions of the gas-phase doublets were in good agreement with the pure gas-phase spectra.

The salt solution in "pure water" contains some adventitious carbon. Even when the salt crystals have been extensively sputtered and the dry salt shows no surface carbon, the XPS signal from carbon appears upon deliquescence. Ongoing work in our group is investigating the effect of this adventitious carbon. Upon addition of butanol to the solution, the adventitious carbon is displaced from the surface, we assume by dissolution into the solution. For several reasons, we conclude that the surface carbon we measure in the KI−water−butanol solution is butanol and not the adventitious carbon. A portion of the adventitious carbon appears at binding energies that are higher than the butanol carbon signal, and these peaks go away in the presence of butanol. Furthermore, the constraints on the C−O/C−H peak ratios and energy splittings derived from gas-phase butanol spectra fit the carbon spectra from the solution well. When butanol is added, the total carbon coverage on the sample goes down, scatter in the carbon signal decreases significantly, and it becomes a monotonic function of photoelectron kinetic energy. We made the multicomponent solution by two methods as a check to see if the results depend on the manner of solution preparation (see Experimental Procedures). The data from the two methods of making a solution are indistinguishable.

Elemental Ratios. The butanol XPS carbon signal in the ternary mixture is enhanced at the solution surface. The mole fraction of butanol as a function of photoelectron kinetic energy is shown in Figure 2. At lower photoelectron kinetic energies, which give a more surface sensitive signal, the amount of carbon arising from butanol is greater than at high photoelectron kinetic energies, which are more representative of the bulk. This result agrees with previous surface tension[14] and neutron scattering[15] measurements showing that butanol−water mixtures exhibit surface segregation of butanol.

In the absence of butanol, the ratio of iodide to potassium shows a substantial increase near the liquid−vapor interface of a saturated aqueous solution of KI, as published in previous work from this group.[5] The I/K ratios are higher at low photoelectron kinetic energy due to the surface enhancement of the polarizable iodide anions in solution. In the presence of butanol, we observe a dramatic flattening of the depth dependence of the I/K ratio. In Figure 3, we show this effect for solutions made from both of our methods (water and butanol added simultaneously, or water and butanol added sequentially). As shown in Figure 4, we also verified that the change in ion distribution was directly related to the addition of butanol by comparing the I/K ratio before and after the addition of butanol for a given sample.

Despite the suppression of iodide enhancement at the liquid−vapor interface that we observe, the ion signal intensities indicate that there are still substantial amounts of anions and cations at the interface. These data support a picture in which ions still exist at the interface in the presence of butanol, but the anion/cation ratio is now relatively constant as a function of depth into the sample.

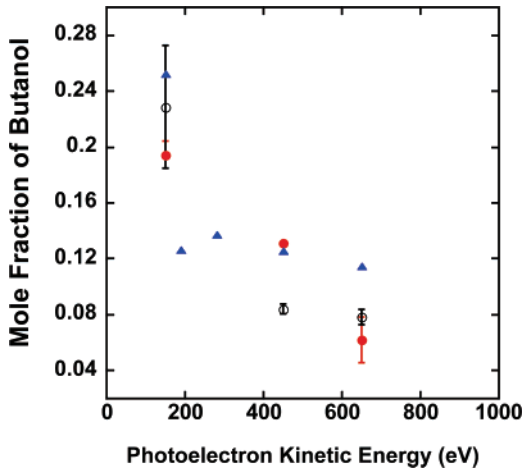

Figure 2. Plot showing the amount of adsorbed carbon on the deliquesced sample in the presence of butanol during three different experiments. The ratio of moles butanol (determined from $C_{adsorbed}$) to total moles of species in solution is shown. The value for total moles of species in solution is determined from the sum of $O_{adsorbed}$ (which arises from both water and butanol) with K and I. Because of low signal, we have no oxygen data at 800 eV photoelectron kinetic energy, but other measures show a continued decrease of carbon at that energy. Error bars show the standard deviation of averaged measurements; their absence indicates that a single measurement is shown. The data in closed and open circles were taken in the same month, whereas the data in triangles were taken several months later. The data correspond to gas-phase butanol/water ratios of 0.06 (closed and open circles) and 0.02 (triangles). We have indications that the main difference in signal between the data in circles and the data in triangles is due to deviations in the photon flux measurements.

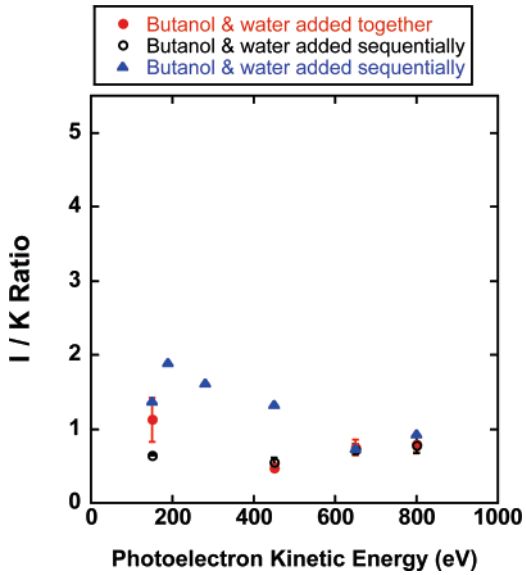

Figure 3. Plot showing the ratio of I to K composition as a function of photoelectron kinetic energy during three experiments. We find similar results when the butanol is added before and after deliquescence of the salt. When given, error bars show the standard deviation about an average value from repeated measurements. The data in closed and open circles were taken in the same month, whereas the data in triangles were taken several months later. The data correspond to gas-phase butanol/water ratios of 0.06 (closed and open circles) and 0.02 (triangles). We have indications that the main difference in signal between the data in circles and the data in triangles is due to deviations in the photon flux measurements.

To determine the gas-phase butanol concentrations in these experiments, we compared the gas-phase oxygen photoelectron signal from water and butanol. This measure gives a butanol−water mole ratio ranging from 0.02 to 0.06 for the data presented

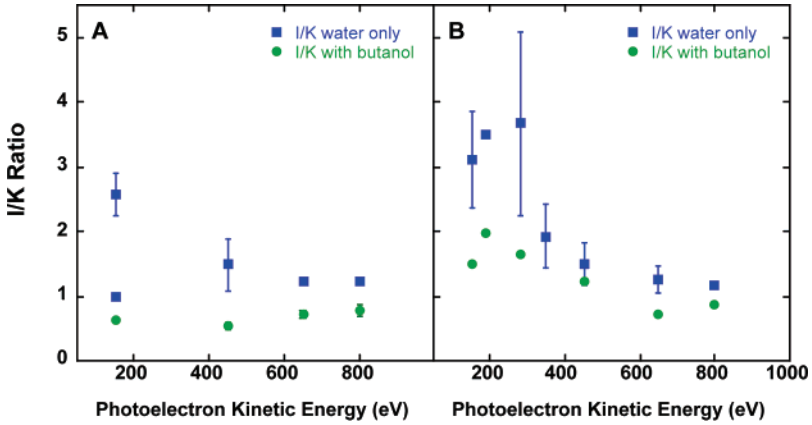

Figure 4. Plot showing the ratio of I to K integrated areas for water and butanol added sequentially during solution preparation. We show ratios before and after the addition of butanol, demonstrating the decrease in the I/K ratio at low photoelectron kinetic energy with addition of butanol. Butanol/water mole ratios are (a) 0.06 and (b) 0.02. When given, error bars show the standard deviation about an average value from repeated measurements.

here. The total pressure was also monitored at all times with a baratron. However, once the gas mixture is in the chamber, the baratron cannot measure the butanol and water separately, so the XPS data provide the best measure of the gas-phase concentration. The absolute pressure measurements from the baratron are used to calculate the relative humidity in the chamber.

It is more difficult to ascertain the solution-phase concentration of butanol. If we use the 298 K Henry's law constant of butanol,[18] we arrive at solution-phase concentrations ranging from 0.02 to 0.007 M. Two factors ensure that this estimate is an upper bound on the solution-phase concentration. The Henry's law constant will be reduced at lower temperatures but because the solution and the vapor are not at the same temperature in this experiment, the magnitude of this reduction is unclear. Because KI is a salting-out agent for butanol, we expect butanol to be less soluble and more surface active in the presence of KI but were unable to find literature data about the effect of KI on the butanol−water Henry's constant. To explore the effect of KI on the surface concentration of butanol, we performed a series of surface tension measurements, reported in the next section.

B. Surface Tension. As previously mentioned, the interfacial activity of 1-butanol in aqueous solutions has been widely studied by surface tension measurements,[14] neutron reflectivity experiments,[15] and computer simulations.[16] It is understood that KI acts as a salting-out agent when added to a butanol−water solution.[19] However, we have not found any published quantitative studies of the interfacial concentrations in KI−water−butanol solutions. To characterize the impact of salt on the surface concentration of butanol in our ambient pressure XPS measurements, we measured the surface tension of solutions of saturated KI with several concentrations of butanol. Results are shown in Figure 5a as a plot of γ versus butanol concentration. These data are fit to a Langmuir model in which

$$\gamma = \gamma_0\left\{1 - B\ln\left(\frac{c_{\text{butanol}}}{A} + 1\right)\right\} \qquad (1)$$

where c_{butanol} is the molar concentration of butanol and A and B are fitting parameters with $A = 0.037$ M and $B = 0.19$ for saturated KI solution, and $A = 0.0031$ M and $B = 0.16$ for saturated KI with butanol added. For KI−water−butanol solutions, γ_0 is the surface tension of a saturated KI solution, taken to be an average experimental value of 79.3 ± 2 mN/m, and for water−butanol solutions γ_0 is the surface tension of pure water. All values of surface tension are offset so that the surface tension of water is 72.75 mN/m.[44] This corrects for a systematic error in the measurements that is likely due to a slight change in the contact angle for plates that have been exposed to salt solution. For butanol concentrations of 0.18 M and above, phase separation of the ternary KI−water−butanol solution was

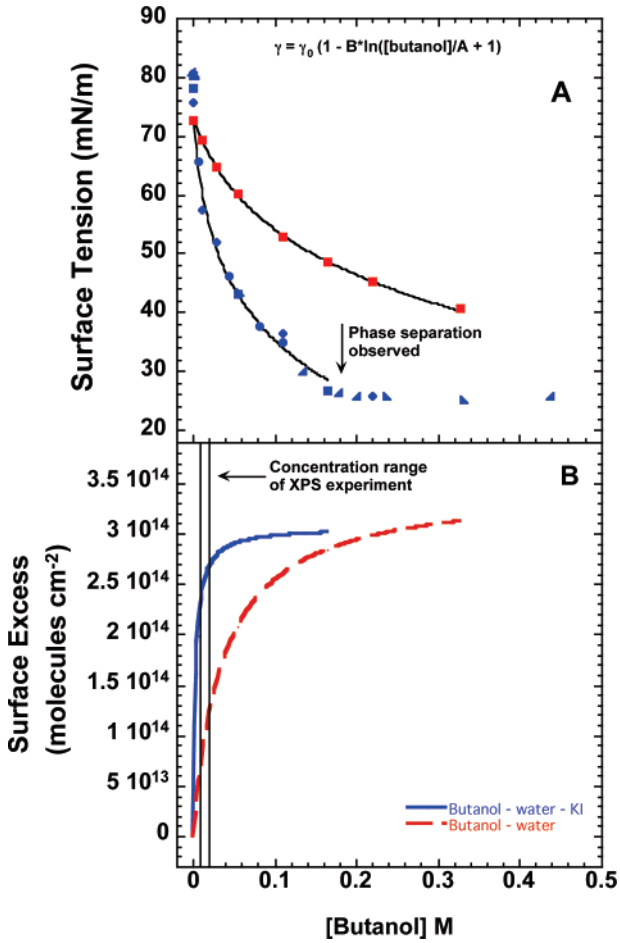

Figure 5. Surface tension measurements for butanol in water (red squares) and for saturated aqueous KI solutions (blue symbols) are given in panel a. The KI−water−butanol data were taken from five different solutions of KI; data points from a given solution are shown with the same symbol (squares, circles, diamonds, and right or left triangles). The fit through the data is described by eq 1 and gives the coefficients noted on the text. The derivative of that function is used in eq 2 to calculate the surface excess values shown in panel b.

observed. Accordingly, the butanol concentrations that correspond to surface tension measurements in this range have large associated uncertainties. Only data at butanol concentrations below 0.18 M are used to fit the data via eq 1, but this region includes most of the total rise in surface excess.

We are interested in the surface excess of butanol, as defined by

$$\Gamma_{\text{butanol}}^{\text{KIsolution}} \approx \frac{-a_{\text{butanol}}}{RT}\left(\frac{\partial\gamma}{\partial a_{\text{butanol}}}\right)_{T,\mu_{\text{KI}}} \approx \frac{-c_{\text{butanol}}}{RT}\left(\frac{\partial\gamma}{\partial c_{\text{butanol}}}\right)_{T,\mu_{\text{KI}}} \quad (2)$$

Here $\Gamma_{\text{butanol}}^{\text{KIsolution}}$ is the surface excess of butanol at a given salt concentration relative to the surface excess of saturated KI solution. Equation 2 assumes that activity changes linearly with concentration. While a linear fit predicted activities with under 5% error for the data from Harkins and Wampler[14] for butanol−water solutions up to 0.5 M in butanol, deviations from linearity in the presence of salt should be larger. We also assume that the chemical potential of KI is not changing appreciably as the butanol is added to the solution. Using the derivative $(\partial\gamma/\partial c_{\text{butanol}})_{T,\mu(\text{KI})}$ from the fit in eq 1, we calculate $\Gamma_{\text{butanol}}^{\text{KIsolution}}$; the result is plotted in Figure 5b as a function of concentration. The presence of KI has a clear salting-out effect on butanol, which is consistent with previous experiments on ternary KI−water−butanol solutions.[19] For butanol−water solutions, the surface excess approaches its maximum value at significantly higher concentrations. To quantify this difference, we use a different expression of the Langmuir model:

$$\Gamma = \Gamma_{\text{sat}}\left(\frac{c_{\text{butanol}}}{b + c_{\text{butanol}}}\right) \quad (3)$$

We find that $\Gamma_{\text{sat}} = 3.0 \times 10^{14}$ molecules/cm^2 with $b = 0.0031$ for KI−water−butanol solutions and $\Gamma_{\text{sat}} = 3.5 \times 10^{14}$ molecules/cm^2 with $b = 0.037$ for butanol−water solutions. Because the $\Gamma_{\text{butanol}}^{\text{KIsolution}}$ values depend on the derivative of the surface tension data, they are highly sensitive to the fit. While the shape of the surface excess curves show robust differences between the aqueous KI solutions with and without butanol, the differences in Γ_{sat} are not likely to be significant. For the ternary KI−water−butanol solution, we reach 87% of Γ_{sat} at a butanol concentration of 0.02 M, close to a saturated surface layer of butanol. For the butanol−water solution, we reach 35% percent of the Γ_{sat} value for butanol at the same solution concentration. The observation that the addition of salt to surfactant solutions produces a more rapid decrease in surface tension with increasing surfactant concentration has also been seen in other work.[45]

Our surface tension experiments provide a measure of the butanol surface excess. We are more interested in the total butanol surface concentration. However, at the low bulk concentrations of butanol used in our experiments, the total surface butanol concentration is within 1% of the surface excess, as can be shown using the approach described by Torn and Nathanson.[46] On the basis of our surface tension measurements, the range of butanol concentrations at the liquid−vapor interface in our ambient pressure XPS experiments is $(2-3) \times 10^{14}$ molecules/cm^2.

C. MD Simulations. *Density Profiles.* The vertical density profiles of ions, water, and alcohol resulting from MD simulations for the systems containing a total of 32, 50, 72, and 98 1-butanol molecules (i.e., roughly half of these numbers per interface) are shown in Figure 6, along with snapshots of the top and side views of the corresponding slabs. As the concentration of 1-butanol molecules increases, the pronounced interfacial and subinterfacial peaks of I^- and Na^+, respectively, decrease in intensity until they eventually disappear. However, Figure 6 also clearly shows that both ions are present at the interface at all alcohol coverages, for their concentration is significant above the Gibbs dividing surface of all the systems considered. At the largest alcohol coverage (Figure 6D), the concentrations of both kinds of ions become comparable throughout the slab with no anion segregation at the interface. Hence, the presence of butanol favors a situation where the two ion species are found at the interface with similar concentrations, in contrast to when no alcohol is present (or present at low concentrations) and in which case the ions form a double layer at the interface as stated above. The density profiles have been normalized so that the bulk value of the water and the ions, as well as the maximum value of the alcohol, is one (note that this normalization process magnifies the ion density profiles by approximately a factor of 10 with respect to the water density profile because the ratio of water to ion pairs is close to 10).

The top views of snapshots of the slabs on the left column of Figure 6 show that only for the largest alcohol coverage (∼49 1-butanol molecules per side) does the alcohol appear to cover the liquid surface uniformly, but even in this case the packing is still loose. In both the top and the side views, we see that the alcohol molecules are highly disordered, and they tend to penetrate the interface via the formation of local pockets. Furthermore, as expected, the alcohol behaves mostly as a surfactant. In the systems containing 72 and 98 1-butanol molecules, we occasionally observed a 1-butanol molecule entering the bulk solution and becoming completely solvated. Given the relatively small system sizes and simulation times, the sampling of bulk 1-butanol configurations is too limited for a detailed analysis, so we will restrict our attention to 1-butanol molecules on the surfaces of the solutions. We calculate the surface coverage of 1-butanol molecules for the 32, 50, 72, and 98 butanol slabs to be 1.8×10^{14}, 2.8×10^{14}, 4.0×10^{14}, and 5.4×10^{14} molecules/cm^2, respectively. This places our estimate of the experimental surface coverages in the same range as the simulations.

Figure 7 shows the ratio of the cumulative densities of iodide anions to sodium cations computed as

$$P_{I^-}(z)/P_{Na^+}(z) = \int_z^{z_{\text{top}}} \rho_{I^-}(z')\,dz' / \int_z^{z_{\text{top}}} \rho_{Na^+}(z')\,dz' \quad (4)$$

where z_{top} is the value of z at the top of the slab, and ρ_{ion} is the density profile of the given ion symmetrized with respect of the center of the slab. To enable a direct comparison of all of the systems, in Figure 7 the vertical axis of each system has been translated so that the $z = 0$ coincides with the Gibbs-dividing surface (i.e., the point for which the density of water has reached half of its bulk value). Note that $z < 0$ corresponds to the bulk phase of the solution, and $z > 0$ to the vapor. The curves clearly show an enhancement of anions (anion/cation ratios significantly greater than unity) in the interfacial region ($z > 0$) of the neat NaI solution and the solutions with a low coverage of 1-butanol (i.e., the systems with 32 and 50 1-butanol molecules). In going from the system with no alcohol present to the systems with 32 and 50 1-butanol molecules, we notice only a small change in the overall shape of the curves and a slight reduction in the interfacial anion enhancement. For the system containing 72 1-butanol molecules, the curve appears to flatten out, and it is almost completely flat for the system

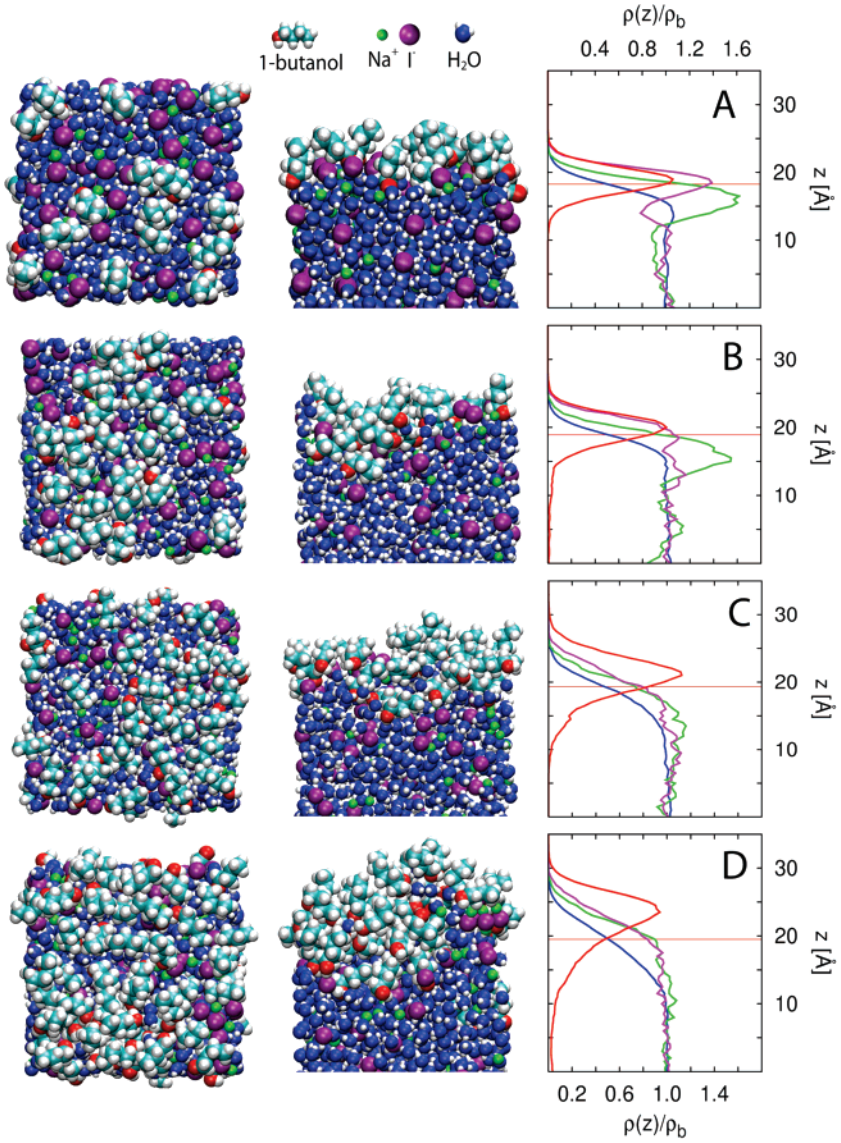

Figure 6. Snapshots of the simulation (left column, top view; middle column, side view) and the corresponding density profiles (right column). From top to bottom the systems are: 5 M NaI aqueous solutions containing $n = 32$ (A), 50 (B), 72 (C), and 98 (D) 1-butanol molecules (with roughly $n/2$ per interface). The colors of the density profiles correspond to the coloring of the atoms in the snapshots (red for 1-butanol O atoms, blue for water O, purple for the iodide ion, and green for the sodium ion). The red line denotes the position of the Gibbs-dividing surface, which is the point at which the water density is half its value in the bulk solution.

with 98 1-butanol molecules. This result qualitatively agrees with the experimental measurement of flat I/K ratios in the presence of butanol, and the previously reported enhanced surface anion/cation ratios in the absence of butanol.[5]

The data shown in Figure 7 reveal a drop in the interfacial anion enhancement in the system containing 72 1-butanol molecules as compared to lower butanol concentrations. The number of alcohol molecules per interface in that system (~36) corresponds to the average number of iodide ions in the interfacial area of the neat 5 M NaI aqueous solution slab. This suggests that the reduction in the interfacial enhancement of anions that accompanies the addition of 1-butanol could be due to specific interactions between the alcohol molecules and the ions. Indeed, it is evident in Figure 6 that the suppression of the interfacial ion enhancement corresponds to a migration of the ions toward the interior of the solution where they can participate in interactions with the hydrophilic alcohol heads, which are well solvated.

Surface Tension. We have computed the surface tension of the water−butanol system as a way of validating the force field employed in this study. Assuming that the butanol surface concentration is equivalent to its surface excess, as discussed in the experimental surface tension discussion, we have estimated the molarity corresponding to the surface excess from eq 3 (for the system containing 16 and 25 alcohol molecules per side) or from Li et al.[15] (for the system containing 36 molecules per side). A comparison of the computed and experimental surface tension data is presented in Figure 8. Note that the concentration of the system containing 49 molecules per interface is out of the range of the experimental measures and is therefore not reported. At the concentrations corresponding to no butanol and the lowest butanol coverage studied here (corresponding to 0.04 M), we observe the largest deviations of the computed surface tension from the experimentally determined data. This deviation is due to the model used for water in the current study (POL3[40]), which underestimates the surface tension of pure liquid water. Overall, the comparison shows that the force field used for the butanol can reproduce the concentration dependence of surface tension for the water−butanol system, and hence that the butanol−butanol and

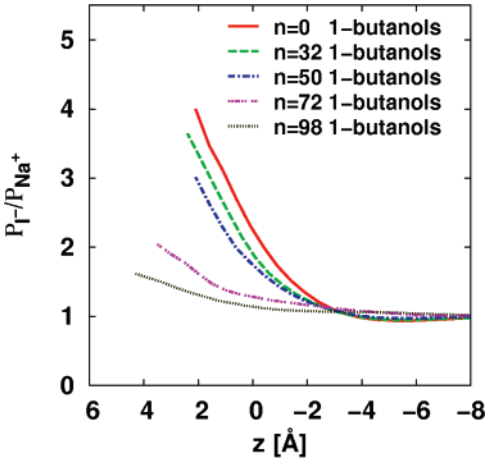

Figure 7. Ratio of the cumulative densities of I^- and Na^+ for the five systems studied, plotted as a function of the displacement relative to the Gibbs dividing surface ($z = 0$). The ratio is a measure of the preferential adsorption of iodide at the interface and goes to unity beneath the surface ($z < 0$), as expected for a bulk monovalent salt solution. The ratios given here do not incorporate information about the experimental probe depth.

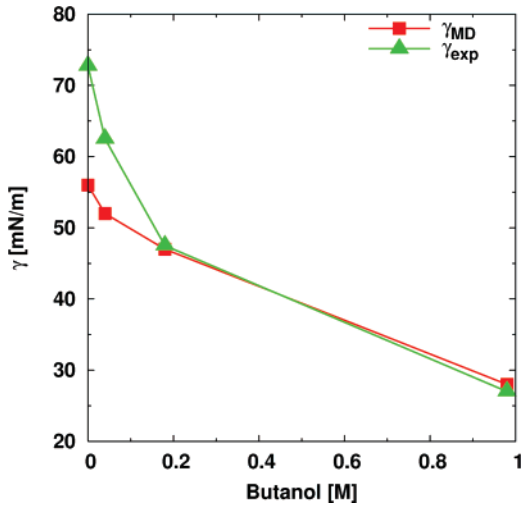

Figure 8. Comparison of the surface tension computed, γ_{MD}, and experimentally determined, γ_{exp}. The three experimental data points at the lower concentrations are from the current work and the surface tension value at the highest concentration is from Addison.[47]

butanol−water interactions are reasonably well balanced, especially at the higher butanol concentrations.

Radial Distribution Functions. To quantitatively characterize butanol−ion interactions, we have evaluated the radial distribution functions (RDFs) of ions around the alcohol molecules in the interfacial region (Figure 9). In the butanol O−Na^+ RDF, there is a sharp peak at 2.3 Å, indicating a strong interaction. The corresponding running coordination number shows that on average ∼0.2 sodium cations are paired with the hydrophilic head of the alcohol. There is also evidence of a weaker, but well-defined, second shell of sodium in the vicinity of the butanol hydroxyl groups. The peak at 2.7 Å in the butanol H_{OH}−I^- RDF, corresponding to a direct interaction of I^- with the hydroxyl hydrogen of 1-butanol, is not as pronounced as the first peak in the butanol O−Na^+ RDF. The running coordination number gives again ∼0.2 iodide anions directly interacting with the hydroxyl group of the alcohol. There is also evidence of a second shell of iodide anions around the butanol hydroxyl groups.

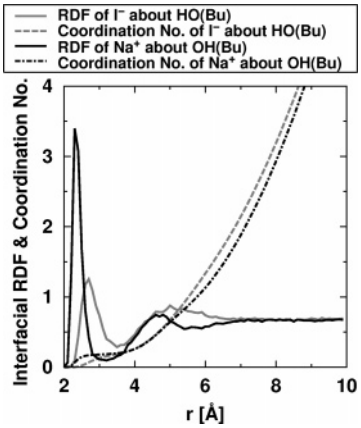

Figure 9. Interfacial radial distribution functions and corresponding running coordination numbers for the sodium cation (solid and dot−dashed black lines) around the 1-butanol oxygen atom and for the iodide anion (solid and dashed gray lines) around the 1-butanol hydroxyl hydrogen atom in the system containing 72 1-butanol molecules. Note that the RDFs do not converge to unity in the anisotropic interfacial region.

TABLE 1: Number of Alcohol Molecules That Interact Directly with Na^+ and I^-[a]

	no. of alcohol molecules that interact directly with	
alcohol coverage	Na^+	I^-
32 butanol molecules	6.8	8.0
50 butanol molecules	9.2	9.7
72 butanol molecules	11.2	11.5
98 butanol molecules	11.3	12.1

[a] The numbers were obtained as an average over a 1 ns trajectory for each simulation.

The butanol−ion coordination numbers are less than one because at any given time only a fraction of the total number of alcohol molecules are interacting directly with an ion. The number of alcohol molecules that interact directly with ions is given in Table 1 for the different amounts of alcohol coverage considered. The number of butanol molecules directly interacting with a cation or an anion appears to converge to the values of 11 and 12, respectively, when a total of 72 butanol molecules are present (i.e., 36 per interface). Considering that only a fraction of the total number of butanol molecules are at any given time interacting with each type of ion, a better measure of direct butanol−ion interactions is the number of ions contained in the first solvation shell about an alcohol molecule when it is interacting with an ion. We find that the number of Na^+ or I^- contained in the first solvation shell about the OH group of butanol molecules directly interacting with ions is ∼1, as expected.

We have also looked at how ion pairing changes in the system containing 98 1-butanol molecules compared to the neat 5 M NaI solution. The RDFs of I^- around Na^+ for the two systems are presented along with the corresponding running coordination numbers in Figure 10. In the neat NaI solution, about two iodide ions are directly interacting with each sodium cation in the interfacial region, while ∼0.5 I^- ions are pairing with Na^+ in the bulk (defined as the region for which $|z| < 8$ Å). Ion pairing is slightly reduced in the presence of 1-butanol where ∼1.5 I^- ions are interacting with each Na^+ at the interfacial region. The interfacial area has been defined here as the region contained between the water Gibbs−dividing surface and the height at which the density of water has decayed to 10% of its bulk value. In this region, in the case of a neat NaI solution the iodide ion

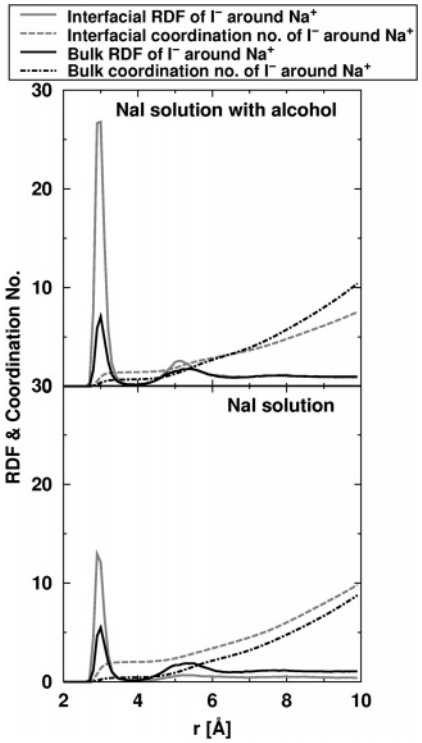

Figure 10. Radial distribution functions for I^- around Na^+ for the system containing 98 1-butanol molecules (top panel) and for the 5 M NaI aqueous solution (bottom panel).

concentration is roughly double that in the bulk. Therefore, the anions tend to pack more closely than in the rest of the slab so that more than one I^- can interact directly with its counterion Na^+ (as would be expected in a traditional ion-pairing situation). In the bulk of the slab, the coordination number of iodide ions in the first solvation shell of sodium cations is ~0.5. The reduction in ion pairing in the presence of butanol is due to the overall reduction in the interfacial concentration of anions. For both systems (with and without alcohol), ion pairing is more prevalent at the interface (solid gray curve) compared to the bulk. In the case of the neat ~5 M NaI aqueous solution, this is mostly due to the formation of a double layer consisting of a layer of iodide adsorbed to the surface and a subsurface layer of sodium counterions. In the presence of 98 1-butanol molecules where interfacial anion enhancement is largely suppressed, the increase in ion pairing at the interface is due to the fact that the alcohol hydroxyl groups draw anions and cations into the vicinity of one another, where they can favorably interact simultaneously with each other as well as the alcohol.

Surface Orientational Ordering. We utilize two related quantities to quantify the orientational order of water and butanol molecules, the polar order parameter, $S(z) = < \cos\theta >$, and an orientational order parameter defined as the average of the second Legendre polynomial, $P(z) = (1/2) < 3\cos\theta^2 - 1 >$, where θ is the angle formed between a vector normal to the air−liquid interface (the *z*-axis) and a vector antiparallel to the water dipole (i.e., along the H−O−H bisector, directed from the positive hydrogen side to the negative oxygen). $S(z)$ provides detailed information on the polar orientation order because it is proportional to the average vertical component of the water molecule dipole moments. A negative value of $S(z)$ indicates that the vertical components of the water dipoles point toward the air on average, while a positive value indicates that the dipoles point into the solution on average, and a value around zero is obtained for an isotropic orientational distribution of water dipoles. Similarly, $P(z) = 0$ represents a system with no net orientation, $P(z) = -1/2$ represents a system with all dipoles parallel to the interface, and $P(z) = 1$ indicates a system with all the water dipoles perpendicular to the interface.[16]

Figure 11 shows the behavior of the two order parameters as functions of position in the slab for four representative systems with $n = 0$, 50, 72, and 98 1-butanol molecules. The water and butanol density profiles (solid blue and dashed−dotted cyan lines) are also shown in Figure 11 for reference. In Figure 11A, we see that the water molecules in the neat 5 M NaI aqueous solution (no butanol) have a net orientation at the interface. Specifically, in the outermost layers of the interface the vertical components of the water dipoles point, on average, toward the air. A subsurface layer follows with the dipoles pointing toward the bulk. As alcohol is introduced in progressively larger amounts (Figure 11B−D), we see that the net interfacial water orientation tends to gradually disappear, i.e., $S_w(z)$ and $P_w(z)$ flatten out.

The orientational parameters $S_b(z)$ and $P_b(z)$ for 1-butanol are also plotted in Figure 11B−D. To describe the orientation of the alcohol, we have considered the projection of three distinct vectors along the vertical direction, *z*. Two of these vectors connect two nonadjacent carbons, while the third connects the methyl carbon to the hydroxyl oxygen. The $S_b(z)$ and $P_b(z)$ computed using these three vectors are, within statistical noise, identical, and this demonstrates that on average the alcohol forms a layer of straight chains with the hydrophilic OH group pointing toward the interface. The progressive disappearance of the preferential orientation of water at the interface as the alcohol is introduced is a signature of disorder resulting from disruption of the water hydrogen-bond network. From the perspective of the water molecules, the presence of the alcohol hydroxyl groups with which the water can hydrogen bond softens the transition from the bulk to the gas phase, thus flattening out the net interfacial orientation.

Discussion

The increased iodide/potassium ratio at the liquid−vapor interface observed in aqueous KI solutions is suppressed upon the addition of butanol, as seen in I/K ratios from experiments and MD simulations. The analysis of the MD trajectories in terms of density profiles, radial distribution functions, and orientational order parameters suggests two reasons for the reduction of the interfacial ion segregation. We find that the flattening of the I/K profile is due to (i) the strong interaction between the 1-butanol molecules and both ions, and (ii) the fact that the alcohol molecules for the most part sit on the interface with their OH groups pointing toward the bulk of the solution, so that ions are displaced away from the organic-vapor interface to interact directly with the alcohol hydroxyl groups. Moreover, the orientational preference of water molecules at the neat water−air interface, observed when no alcohol is present, is modified in the presence of 1-butanol. As the water orientational preference in neat water is predisposed toward solvating a double layer at salt−water interfaces,[48] its alteration is presumably correlated with the reduction in the interfacial anion enhancement. A cartoon illustrating the orientation of butanol on the solution surface and the interaction of the anions and cations with the OH on butanol is shown in Figure 12.

Previous work on salt−water−butanol mixtures also suggested that salt can interact with butanol. Liquid−liquid equilibrium studies by Al-Sahhaf et al. examined ternary solutions of water, butanol, and salt (KI, NaBr, or LiCl), in concentration ranges where the mixtures underwent phase separation into two liquid phases.[19] The authors conclude

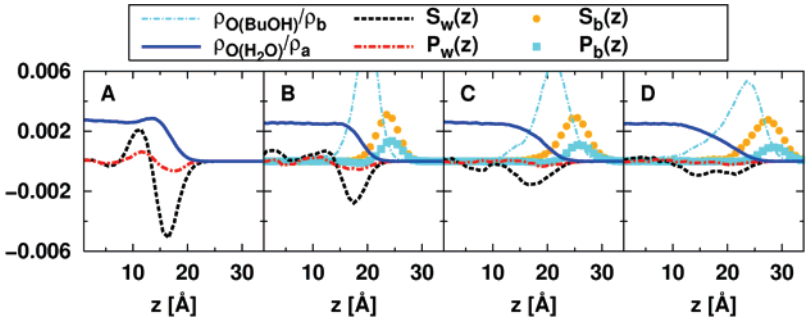

Figure 11. Orientational order parameters of water ($S(z)$ dashed black line, $P(z)$ dashed−dotted red line) and 1-butanol molecules ($S(z)$ orange circles, $P(z)$ cyan squares) are plotted along with the water oxygen density profile (solid blue line) and the 1-butanol oxygen density profile (thin dashed−dotted cyan line). Panel A, neat 5 M NaI aqueous solution; B, 50 1-butanol coverage; C, 72 1-butanol coverage; and D, 98 1-butanol coverage. Note that ρ_a/ρ_b is proportional to the ratio of the total number of water to the total number of 1-butanol molecules.

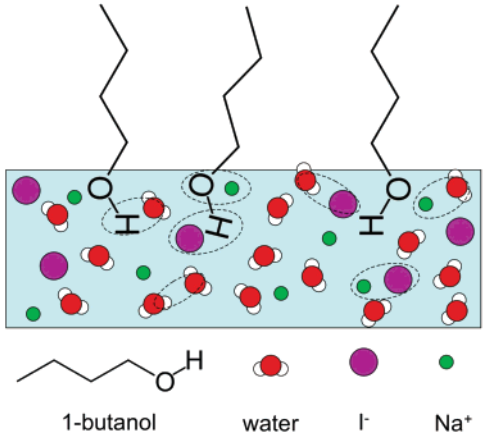

Figure 12. A cartoon showing the liquid−vapor interface of a KI−water−butanol solution. In pure KI−water solutions, the anion concentration is enhanced at the interface as a result of stabilization due to polarization. In contrast, in the presence of the surface-active butanol, specific ion−alcohol interactions result in both the anion and the cation residing at the interface. Dashed lines encompass representative interactions possible in the solution.

from their data that the KI−water−butanol system exhibits cosolvation of the salt by both water and butanol with the solvation equilibrium shifting as a function of solution composition. Solvation behavior was highly dependent on the identity of the salt. Although the salt appeared to be cosolvated by both water and butanol when it was KI or LiCl, in solutions where KBr and NaBr were examined the salt was mainly solvated by water. Wakisaka et al. used mass spectrometry to look at which species clustered together upon thermospray and electrostray ejection from water−butanol−salt solutions, as well as mixtures of water and butanol.[49] They found evidence for preferential solvation of the cations (which included K^+) by butanol instead of water. While the anion, Cl^- was preferentially solvated by water, it was also solvated by butanol to a lesser degree. This past work is consistent with our mechanistic picture in which specific butanol−salt interactions strongly affect interfacial structure.

The results of the MD simulations are also consistent with previous computational work on similar systems. Our MD simulations show interfacial water and butanol orientational parameters similar to those observed by Chen et al. for a binary butanol−water system.[16] Wardle et al. examined the liquid−liquid interface of a ternary 1-hexanol−water−NaCl solution with MD simulations using a nonpolarizable force field for the water and the ions.[50] Although those authors examined a liquid−liquid interface instead of a liquid−vapor interface, they observed a similar orientation of the hexanol OH headgroups pointing toward the aqueous phase as we observe for butanol. They also found that net solvation of the salt ions decreased in the interfacial region, which they attributed to the salt interacting with the hexanol and disrupting the hydrogen-bonding network of interfacial water. They observed the formation of an electrical double layer of salt near the interface, which they attributed to the interaction of chloride anions with the hydrogens of the alcohol OH groups oriented toward the interface. Daiguji performed a MD simulation on aqueous LiBr solutions containing three types of alcohol: *n*-propanol, *n*-heptanol, and *n*-undecanol.[51] He found that salt increases the surface excess concentration of the adsorbed layer of the alcohols (salting-out effect) and that the interaction among the hydrophobic parts of the long hydrocarbon chain alcohols are strong so that the hydroxyl groups do not always point toward the interface.

One lesson we draw from this work is that extrapolating from observed ion surface enhancement in aqueous electrolyte solutions to a predicted impact on atmospheric aerosol chemistry is likely to be a complex process. Experimentally, we observe that the surface-active organic butanol can completely suppress enhancement of the anion/cation ratio at the interface. However, even in the presence of butanol, the absolute ion concentrations are still significant in the interfacial region, as shown in Figure 6C,D. Thus we anticipate that reactions of impinging molecules with ions at the interface will still be significant in the presence of butanol. Indeed, trapping of oxidants by the organic surface layer can increase heterogeneous reaction rates, as was shown for a model organic on water in previous work from our group.[52] Ions interacting with the butanol OH are close enough to the interface that they are likely to be accessible for reaction. Depending on its structure, it is possible that the butanol layer is quite permeable to incoming gases. There is strong experimental evidence that butanol forms permeable films on sulfuric acid solutions. Lawrence et al. found that adding up to 80% of a saturated butanol monolayer did not decrease water evaporation from sulfuric acid within experimental uncertainty.[53] Although this result may be linked to the presence of the sulfuric acid and its capacity to react with butanol,[46] the possibility that butanol may form permeable films on water or saturated KI solutions cannot be discounted. The effect of butanol films upon reaction rates of gas with the sulfuric acid is dependent on chemical identity; butanol enhanced reaction rates of HCl and DCl with sulfuric acid but inhibited N_2O_5 hydrolysis.[54,55]

We expect that the effects observed in this study will apply to a wide range of salt concentrations, but confirmation of this hypothesis requires further study. Some portion of atmospheric aerosols fall into the highly concentrated salt regime directly studied in this paper. At relative humidities commonly present in the atmosphere, many aerosols are present as suspensions of

solid salt particles. As the humidity increases, these particles are coated with thin layers of concentrated salt solution before they eventually deliquesce. The concentrations of organics investigated in this experiment also fall into an atmospherically relevant range. Recent studies have observed aerosol particles in the atmosphere that contain mass fractions of organic compounds much higher than those used in this experiment.[56] Demou and Donaldson point out that salting-out effects should link aerosol salt concentrations and the degree of organic coatings present on aerosol particles, leading to decreased organic coatings due to atmospheric uptake but increased organic coatings that originate from nonvolatile organic species in seawater.[45] Aerosol composition is known to vary widely with location and aerosol size, but the prevalence of aerosols with both salt and organic concentrations in the range examined by this paper is not well characterized.

The importance of specific ion effects for understanding the structure of aqueous electrolyte solutions has been increasingly recognized in recent years.[4] Qualities such as polarizability and local solvation have proven crucial to determining the structure at the liquid−vapor interface of solutions. Here, we encounter an example in which specific ion interactions dominate the structure and local composition of the liquid−vapor interface of a ternary solution. Our simulations suggest that the suppression of enhancement of the anion/cation ratio at the interface experimentally observed in this study is closely linked to the identity of the organic and the nature of its interaction with salts in solution. Whether or not surface enhancement is observed in ternary solutions is likely to depend on the identity of both the salt and the organic in the mixture. It is possible that certain organics may even increase the relative surface enhancement of ions. For example, the results of a recent X-ray reflectivity study of the charged surfactant dihexadecyl hydrogen phosphate suggest enhancement of the cation over the anion near the liquid−vapor interface of a CsI solution in the presence of the surfactant.[57] Understanding not only the surface composition of organics on aerosols but also the way in which these organics interact with salts will be necessary to develop a clear picture of the reactivity of halide ions at aerosol interfaces.

Acknowledgment. This work was supported by the AirUCI Environmental Molecular Sciences Institute under Grants CHE0431312 and CHE0209719 from the National Science Foundation. The ALS and the Molecular Environmental Science Beamline are supported by the Director, Office of Science, Office of Basic Energy Sciences, Division of Chemical Sciences, Geosciences, and Biosciences and Materials Sciences Divisions of the U.S. Department of Energy at the Lawrence Berkeley National Laboratory under contract DE-AC03-76SF00098. M.A.B. acknowledges support from an ALS Doctoral Fellowship. The authors thank Michael Dennin, Robert Walder, and Kapil Krishan for allowing us to use their equipment and expertise for the surface tension measurements. We are indebted to the Institute for Surface and Interface Science for facilitating collaboration with the Dennin group. We also appreciate Ed Wong's assistance with equipment design at the beamline.

References and Notes

(1) Donaldson, D. J.; Vaida, V. *Chem. Rev.* **2006**, *106*, 1445.
(2) Hu, J. H.; Shi, Q.; Davidovits, P.; Worsnop, D. R.; Zahniser, M. S.; Kolb, C. E. *J. Phys. Chem.* **1995**, *99*, 8768.
(3) Knipping, E. M.; Lakin, M. J.; Foster, K. L.; Jungwirth, P.; Tobias, D. J.; Gerber, R. B.; Dabdub, D.; Finlayson-Pitts, B. J. *Science* **2000**, *288*, 301.
(4) Jungwirth, P.; Tobias, D. J. *Chem. Rev.* **2006**, *106*, 1259.
(5) Ghosal, S.; Hemminger, J. C.; Bluhm, H.; Mun, B. S.; Hebenstreit, E. L. D.; Kettler, G.; Ogletree, D. F.; Requejo, F. G.; Salmeron, M. *Science* **2005**, *307*, 563.
(6) Petersen, P. B.; Saykally, R. J. *J. Phys. Chem. B* **2006**, *110*, 14060.
(7) Petersen, P. B.; Saykally, R. J. *Chem. Phys. Lett.* **2004**, *397*, 51.
(8) Liu, D.; Ma, G.; Levering, L. M.; Allen, H. C. *J. Phys. Chem. B* **2004**, *108*, 2252.
(9) Raymond, E. A.; Richmond, G. L. *J. Phys. Chem. B* **2004**, *108*, 5051.
(10) Winter, B.; Faubel, M. *Chem. Rev.* **2006**, *106*, 1176.
(11) Pegram, L. M.; Record, M. T. J. *Proc. Nat. Acad. Sci.* **2006**, *103*, 14278.
(12) Ghosal, S.; Brown, M. A.; Mun, B. S.; Bluhm, H.; Salmeron, M.; Jungwirth, P.; Hemminger, J. C. To be submitted for publication, 2007.
(13) Jungwirth, P.; Tobias, D. J. *J. Phys. Chem. B* **2002**, *106*, 6361.
(14) Harkins, W. D.; Wampler, R. W. *J. Am. Chem. Soc.* **1931**, *53*, 850.
(15) Li, Z. X.; Lu, J. R.; Thomas, R. K.; Rennie, A. R.; Penfold, J. *J. Chem. Soc., Faraday Trans.* **1996**, *92*, 565.
(16) Chen, B.; Siepmann, J. I.; Klein, M. L. *J. Am. Chem. Soc.* **2002**, *124*, 12232.
(17) Dynarowicz, P. *Colloids Surf.* **1989**, *42*, 39.
(18) Snider, J. R.; Dawson, G. A. *J. Geophys. Res.* **1985**, *90*, 3797.
(19) Al-Sahhaf, T. A.; Kapetanovic, E. *J. Chem. Eng. Data* **1997**, *42*, 74.
(20) Ellison, G. B.; Tuck, A. F.; Vaida, V. *J. Geophys. Res.* **1999**, *104*, 11.
(21) Gill, P. S.; Graedel, T. E.; Weschler, C. J. *Rev. Geophys. Space Phys.* **1983**, *21*, 903.
(22) Wyslouzil, B. E.; Wilemski, G.; Strey, R.; Heath, C. H.; Dieregsweiler, U. *Phys. Chem. Chem. Phys.* **2006**, *8*, 54.
(23) Li, J.-S.; Wilemski, G. *Phys. Chem. Chem. Phys.* **2006**, *8*, 1266.
(24) Buajarern, J.; Mitchem, L.; Ward, A. D.; Nahler, H. N.; McGloin, D.; Reid, J. P. *J. Chem. Phys.* **2006**, *125*, 114506.
(25) Tervahattu, H.; Juhanoja, J.; Kupiainen, K. *J. Geophys. Res.* **2002**, *107*, D164319.
(26) Tabazadeh, A. *Atmos. Environ.* **2005**, *39*, 5472.
(27) Rusdi, M.; Moroi, Y.; Nakahara, H.; Shibata, O. *Langmuir* **2005**, *21*, 7308.
(28) Moroi, Y.; Rusdi, M.; Kubo, I. *J. Phys. Chem. B* **2004**, *108*, 6351.
(29) Voss, L. F.; Hadad, C. M.; Allen, H. C. *J. Phys. Chem. B* **2006**, *110*, 19487.
(30) Bluhm, H.; Andersson, K.; Araki, T.; Benzerara, K.; Brown, G. E.; Dynes, J. J.; Ghosal, S.; Gilles, M. K.; Hansen, H.-C.; Hemminger, J. C.; Hitchcok, A. P.; Kettler, G.; Kilcoyne, A. L. D.; Kneedler, E.; Lawrence, J. R.; Leppard, G. G.; Majzlam, J.; Mun, B. S.; Myneni, S. C. B.; Nilsson, A.; Ogasawara, H.; Ogletree, D. F.; Pecher, K.; Salmeron, M.; Shuh, D. K.; Tonner, B.; Tyliszczak, T.; Warwick, T.; Yoon, T. H. *J. Electron Spectrosc. Relat. Phenom.* **2006**, *150*, 86.
(31) Ogletree, D. F.; Bluhm, H.; Lebedev, G.; Fadley, C. S.; Hussian, Z.; Salmeron, M. *Rev. Sci. Instrum.* **2002**, *73*, 3872.
(32) Acheson, D. T. Vapor pressures of saturated aqueous salt solutions. In *Humidity and Moisture*; Wexler, A., Ed.; Reinhold Publishing Corp.: New York, 1963; p 521. The value at −10 °C is extrapolated from data at 5−30 °C.
(33) Hård, S.; Johansson, K. *J. Colloid Interface Sci.* **1977**, *60*, 467.
(34) Case, D. A.; Darden, T. A.; Cheatham, T. E., III; Simmerling, C. L.; Wang, J.; Duke, R. E.; Luo, R.; Merz, K. M.; Wang, B.; Pearlman, D. A.; Crowley, M.; Brozell, S.; Tsui, V.; Gohlke, H.; Mongan, J.; Hornak, V.; Cui, G.; Beroza, P.; Schafmeister, C.; Caldwell, J. W.; Ross, W. S.; Kollman, P. A. *AMBER 8*; University of California: San Francisco, CA, 2004.
(35) Benjamin, I. *J. Chem. Phys.* **1991**, *95*, 3698.
(36) Wilson, M. A.; Pohorille, A. *J. Chem. Phys.* **1991**, *95*, 6005.
(37) Berendsen, H. J. C.; Postma, J. P. M.; van Gunsteren, W. F.; DiNola, A.; Haak, J. R. *J. Chem. Phys.* **1984**, *81*, 3684.
(38) Ryckaert, J.-P.; Ciccotti, G.; Berendsen, H. J. C. *J. Comp. Phys.* **1977**, *23*, 327.
(39) Essman, U.; Perera, L.; Berkowitz, M. L.; Darden, T.; Lee, H.; Pedersen, L. G. *J. Chem. Phys.* **1995**, *103*, 8577.
(40) Caldwell, J. W.; Kollman, P. A. *J. Phys. Chem.* **1995**, *99*, 6208.
(41) Cornell, W. D.; Cieplak, P.; Bayly, C. I.; Gould, I. R.; Merz, K. M., Jr.; Ferguson, D. M.; Spellmeyer, D. C.; Fox, T.; Caldwell, J. W.; Kollman, P. A. *J. Am. Chem. Soc.* **1995**, *117*, 5179.
(42) *CRC Handbook of Thermophysical and Thermochemical Data*; Lide, D. R., Kehiaian, H. V., Eds.; CRC Press: Boca Raton, FL, 1994.
(43) Yeh, J. J.; Lindau, I. *At. Data Nucl. Data Tables* **1985**, *32*, 1.
(44) *CRC Handbook of Chemistry and Physics*, 87th ed.; Lide, D. R., Ed.; CRC Press: Boca Raton, FL, 2006−2007.
(45) Demou, E.; Donaldson, D. J. *J. Phys. Chem. A* **2002**, *106*, 982.
(46) Torn, R. D.; Nathanson, G. M. *J. Phys. Chem. B* **2002**, *106*, 8064.
(47) Addison, C. C. *J. Chem. Soc.* **1945**, 98.

(48) Jungwirth, P.; Tobias, D. J. *J. Phys. Chem. B* **2001**, *105*, 10468.
(49) Wakisaka, A.; Mochizuki, S.; Kobara, H. *J. Sol. Chem.* **2004**, *33*, 721.
(50) Wardle, K. E.; Carlson, E.; Henderson, D.; Rowley, R. L. *J. Chem. Phys.* **2004**, *120*, 7681.
(51) Daiguji, H. *J. Chem. Phys.* **2001**, *115*, 1538.
(52) Vieceli, J.; Ma, O. L.; Tobias, D. J. *J. Phys. Chem. A* **2004**, *108*, 5806.
(53) Lawrence, J. R.; Glass, S. V.; Nathanson, G. M. *J. Phys. Chem. A* **2005**, *109*, 7449.
(54) Lawrence, J. R.; Glass, S. V.; Park, S.-C.; Nathanson, G. M. *J. Phys. Chem. A* **2005**, *109*, 7458.
(55) Park, S.-C.; Burden, D. K.; Nathanson, G. M. *J. Phys. Chem. A* **2007**, *111*, 2921.
(56) O'Dowd, C. D.; Faccini, M. C.; Cavalli, F.; Ceburnis, D.; Mircea, M.; Decesari, S.; Fuzzi, S.; Yoon, Y. J.; Putaud, J.-P. *Nature* **2004**, *431*, 676.
(57) Bu, W.; Ryan, P. J.; Vaknin, D. *J. Synchrotron Radiat.* **2006**, *13*, 459.